



UNIVERSITÀ
DEGLI STUDI
DI PADOVA

Università degli Studi di Padova

Padua Research Archive - Institutional Repository

Hybrid Copper-Nanowire-Reduced-Graphene-Oxide Coatings: A Green Solution Toward Highly Transparent, Highly Conductive, and Flexible Electrodes for (Opto)Electronics

Original Citation:

Availability:

This version is available at: 11577/3261099 since: 2018-02-26T16:08:14Z

Publisher:

Wiley-VCH Verlag

Published version:

DOI: 10.1002/adma.201703225

Terms of use:

Open Access

This article is made available under terms and conditions applicable to Open Access Guidelines, as described at <http://www.unipd.it/download/file/fid/55401> (Italian only)

(Article begins on next page)

Hybrid copper nanowire-reduced graphene oxide coatings: a “green solution” towards highly transparent, highly conductive and flexible electrodes for (opto)electronics

Alessandro Aliprandi,^a Tiago Moreira,^{b,c} Cosimo Anichini,^a Marc-Antoine Stoeckel,^a Matilde Eredia,^a Ugo Sassi,^d Matteo Bruna,^d Carlos Pinheiro,^c César A. T. Laia,^b Sara Bonacchi,^a Paolo Samori^{a,}*

Dr. Alessandro Aliprandi, Cosimo Anichini, Marc-Antoine Stoeckel, Matilde Eredia, Dr. Sara Bonacchi, Prof. Paolo Samori
University of Strasbourg, CNRS, ISIS UMR 7006, 8 allée Gaspard Monge, F-67000
Strasbourg, France.
E-Mail: samori@unistra.fr

Dr. Tiago Moreira, Prof. César A. T. Laia
Laboratório Associado para a Química Verde (LAQV), REQUIMTE, Departamento de Química, Faculdade de Ciências e Tecnologia, Universidade Nova de Lisboa, 2829-516 Monte de Caparica, Portugal.

Dr. Tiago Moreira, Dr. Carlos Pinheiro
Ynvisible, Rua Mouzinho de Albuquerque 7, 2070-104 Cartaxo, Portugal

Dr. Ugo Sassi, Dr. Matteo Bruna
Nokia Bell Labs, Broers Building, Cambridge CB3 0FA, United Kingdom

Keywords: graphene, copper nanowires, transparent conductor, electrochromic device, flexible electronics

Abstract

We report a novel green chemistry approach to assemble copper nanowires/reduced graphene oxide hybrid coatings onto any inorganic and organic support. Such films are robust and combine sheet resistances ($< 30 \text{ } \Omega/\text{sq}$) and transparencies in the visible region (transmittance $> 70 \%$) which are rivalling those of indium-tin oxide. These electrodes are suitable for flexible electronic applications as they show sheet resistance change $< 4\%$ after 10,000 bending cycles at a bending radius of 1 cm, when supported on polyethylene terephthalate (PET) foils. Significantly, our wet-chemistry method involves the preparation of dispersions in environmentally friendly solvents and avoids the use of harmful reagents. Such inks are processed at room temperature on wide variety of surfaces by spray-coating. As a proof-of-concept, we demonstrate the successful use of such coatings as electrodes in high-performance electrochromic devices. The robustness of our electrodes is demonstrated by performing several tens of thousands cycles of device operation. Our unique conducting coatings hold potential for being exploited as transparent electrodes in numerous optoelectronic applications such as solar cells, light-emitting diodes and displays.

Transparent conducting films are key component as electrodes in modern opto-electronics and are widely employed for the fabrication of touch screens, flat displays, solar cells and organic light-emitting diodes.^[1-2] Indium tin oxide (ITO) is currently the most widely used transparent conductor because of its high transparency in the visible range combined with its highest conductivity and electrochemical stability.^[3] However, ITO films feature a number of drawbacks: (1) they are mechanically fragile, (2) they can hardly be processed on flexible supports, (3) they are expensive due to the high preparation costs and the scarcity of indium in the earth's crust. Therefore, the development of new, low-cost, stable and large-area transparent electrodes is one of the major challenges in material sciences and engineering.^[4-6] Recently, metallic nanowires (NWs) based on copper or silver have gained considerable attention because of their high electrical conductivity and optical transmittance that are comparable to those of ITO.^[3] Moreover, NWs can be readily dispersed into solution and deposited onto different substrates by spray coating or using a meyer rod^[7], which represent big advantages for industrial production. Among them, copper represents the cheapest alternative since the price of the raw material is almost 2 and 4 orders of magnitude lower than silver and gold, respectively. Recently, a green large-scale hydrothermal synthesis of high-quality copper nanowires (CuNWs) with tunable aspect ratios, relying on the use of non-toxic amino acids, hydrophobic amines and glucose as reducing agent has been reported.^[8-10] Despite the increasing interest in these kinds of nanomaterials as components for opto-electronics, several fundamental problems hinder their practical applicability. In particular, CuNWs exhibit a limited chemical stability due its propensity to undergo oxidation which results in a complete loss of electrical conductivity. To remove this oxide layer, harsh methods are typically employed. These include a post deposition treatment based on high temperature annealing (> 175 °C) in reducing hydrogen atmosphere or annealing-free processes consisting in acid etching^[11] and photonic sintering^[12]. In parallel, a great effort has

been devoted to protect CuNWs from oxidation including nickel alloying^[13] and the use of inorganic shells^[14]. However, the latter approach requires cumbersome additional steps such as atomic layer deposition (ALD)^[15] or the electrodeposition of a metal (Zn, Sn, or In) onto the surface of CuNWs network, followed by oxidation to create a transparent oxide shell^[14]. Moreover, albeit the protection of CuNWs through inorganic (semiconducting or insulating) oxide shell can impart them a good stability, such surface passivation can harm or even completely block the heterogeneous electron transfer making the nanowires no longer suitable as electrodes in electrochemical and other opto-electronic devices.

Graphene has been recently reported as long lasting barrier against oxidation.^[16-17] However, the cost of production of high quality chemical vapor deposition (CVD) graphene sheets and the tedious and expensive transfer process make such approach not suitable for the generation of large-area and low cost electrodes^[18]. Conversely, graphene oxide (GO) has received large attention in the past decade because of its low production cost and its high solubility in polar solvents. GO is almost an insulator which can be reduced thermally (by thermal annealing at 700 °C under inert atmosphere^[19-20]) or chemically (e.g. using reducing agents like hydrazine or ascorbic acid^[19-22]) partially restoring the graphitic structure of graphene, yet yielding a sheet resistance $>1,000 \Omega/\text{sq}$, being one and nearly two orders of magnitude higher than pristine graphene and ITO, respectively. Such characteristics render such reduced-GO inapplicable as electrode for opto-electronics.^[19] Recently, Ruoff et al.^[23] have proposed the use of CuNWs covered by reduced graphene oxide (rGO) as transparent electrodes. However, they have employed a cumbersome several steps approach for preparing these CuNWs/rGO based electrodes. This includes (i) poly(methylmethacrylate) (PMMA) dry transfer to mechanically superpose rGO films on top of CuNWs thereby limiting the large-scale production and leveraging the cost of preparation, (ii) treatment with aggressive chemicals like hydrazine, and (iii) three separated thermal annealing treatments under stringent and

controlled atmospheres to reduce the GO, the CuNWs and the final hybrid structure. Overall, there is a great technological demand to produce highly transparent and highly conductive electrodes using green and low-cost preparation approaches that are potentially suitable for any kind of substrates, making them applicable as transparent electrodes for different types of electronic devices.

In this paper we have devised a straightforward method for the preparation of CuNWs/rGO films which relies on the bottom-up formation of CuNWs suspensions by means of the Maillard reaction^[10] and on the use of commercial GO. These two components are processed in thin-film onto any arbitrary substrate through a three-steps procedure (Figure 1): i) spray deposition of an ethanolic suspension of CuNWs, followed by ii) spray deposition of an ethanolic suspension of GO flakes, and finally iii) simultaneous chemical reduction of the two components film in water at room temperature in the presence of NaBH₄ as reducing agent. The rGO layer coating the CuNWs enables to eliminate any additional treatments such as metal electrodeposition^[14] reducing the cost and the preparation time. Our method makes it possible to produce highly stable transparent electrodes suitable for flexible electronics starting from cheap materials and by using a chemically mild approach. As a proof-of-principle, we have exploited the hybrid CuNWs/rGO electrodes to fabricate high-performance electrochromic devices.

Among several methods reported so far for the synthesis of CuNWs^[7, 24], we have focused our attention on the Maillard reaction^[10] approach since it relies on the use of green reagents and mild conditions that are essential for industrial application. In particular, we have employed CuCl₂ as copper source, octadecylamine as surfactant and capping agent and glucose as reducing agent in water (for details see SI paragraph 1). The produced CuNWs were dispersed in a polar solvent such as EtOH and deposited as thin-film onto a glass substrate by using an airbrush (Step *a* in Figure 1). Figure 2a displays a typical SEM image of CuNWs network. It

shows nanowires with an average diameter of 126 ± 33 nm and a length > 20 μm , corresponding to an average aspect ratio > 150 . As expected, such network showed a very low electrical conductivity (sheet resistance ~ 50 $\text{M}\Omega/\text{sq}$) due to the presence of a thin Cu(II)O passivation layer on the CuNWs surface.

In parallel, we have optimized the formation of spray-coated GO-flakes films starting from a commercially available GO suspension. In agreement with Lee et al.^[25], our rGO films suffer from a poor conductivity (sheet resistance ~ 0.4 $\text{M}\Omega/\text{sq}$) hindering their use as electrodes. Interestingly, the use of the airbrush technique allowed us to easily tune the amount of material deposited onto the substrate, therefore to have a fine control over the transmittance and the conductivity of the films at will. The nominal average thickness of the hybrid film amounts to 74.7 nm

With the aim of increasing the conductivity of these two components when processed in thin films and simultaneously retaining the high film transparencies, and avoiding strong annealing treatments, we have tested several wet reducing approaches already reported for GO-flakes based films.^[19] Among them, we have found that for our films the use of NaBH_4 water solution was the most effective and less invasive (for more details see SI paragraph 3). In particular, Figure 2b (red dots) reports the effect of such reducing solution to the electrical characteristics of CuNWs network film as a function of the dipping time; interestingly, the sheet resistance of such film measured by four-probe technique dramatically drops of over 6 orders of magnitude, from 45 $\text{M}\Omega/\text{sq}$ down to 30 Ω/sq , when exposed to the NaBH_4 aqueous solution (0.1% w/w, 14 mM) and it reaches a plateau after about 60 min of treatment (see red curve in Figure 2b). Analogously, films of sprayed GO flakes follow a similar reduction kinetic: Figure 2b (blue curve) displays the trend of the optical film transmittance as a function of the reduction time, complying with the well-known increase in darkness of the film upon rGO reduction. The sheet resistance of the resulting rGO film amounted to ~ 0.4

M Ω /sq. Moreover, we have compared the sheet resistance of reduced CuNWs network films vs their transmittance (Figure 2c). As expected, the conductivity of such films increases non linearly with the increase of thickness of the CuNWs network deposited onto substrate^[3] and it reaches 40 Ω /sq with only 10% loss of transmittance, being a value comparable to ITO. These preliminary data confirm not only that it is possible to have a fine control over the formation of CuNWs and GO films by using a spray-coating approach but also, that their conductivity can be effectively increased upon mild chemical treatments such as an exposure to water NaBH₄ solution at room temperature, without dramatically lowering their transmittance. However, these two films separately are not suitable for replacing ITO as conductive electrodes for electronic applications since reduced CuNWs films are not stable over long-time when exposed to air and rGO films do not possess a sufficiently high electrical conductivity.

To tackle this problem, we have designed and developed a pre-assembled two-components film in which GO flakes are spray-coated on top of CuNWs network film previously deposited on any arbitrary support. The successful coating of CuNWs network with GO flakes was confirmed by SEM microscopy that clearly shows the presence of GO flakes on top of CuNWs (Figure 3a). Once assembled, the film was treated by dipping inside an analogous aqueous solution of NaBH₄ at room temperature reported above for the one-component film. Interestingly, we have found that this approach allows to reduce simultaneously both the bottom CuNWs network and the upper GO flakes without any chemical decomposition of the CuNWs, which are perfectly intact (Figure S2) as confirmed by the XPS analysis carried out on the film before and after the treatments (Figure 3b). In particular, after 2.5 hours of immersion in NaBH₄ solution the Cu(II) peaks at 940-945 eV and 965 eV disappear whereas only the typical peaks of metallic Cu at 932 and 952 eV appear. The XPS analysis of C peaks is displayed in Figure 3c: it exhibits a single peak appearing at 284 eV which can be attributed

to sp^2C of rGO while the C-O band at 286 eV paradigmatic of GO decreases significantly. Interestingly, when a different reducing agent is used such hydrazine or ascorbic acid (see table S1 and Figure S1), a fast decomposition of the CuNWs have been observed. Such result can be ascribed to the tendency of other reducing agents such as hydrazine, chlorine ions or ascorbic acids to act as ligands for the copper cations leading to dissolution and re-precipitation of the metallic copper, ultimately resulting in degradation of the nanowire structure. As far as the optical properties of the reduced CuNWs/GO film, UV-Vis measurements exhibit a loss of about 10 % of the film transmittance after the reduction (Fig. S6a), representing a minor change for applications of these conducting films as electrodes in electrochromic devices. Interestingly, we have observed a detachment of the hybrid film from the glass substrate during the reduction process which can be avoided just by pre-treating the substrate with APTES (see Supporting Information for details), while when PET substrate is employed such a detachment was not observed thereby making the use of a binder unnecessary. Furthermore, the resulting hybrid film did not show any loss of conductivity over a period of three months in air equilibrated conditions at room temperature (Figure S3). The ionization energy (IE) of the reduced two-components CuNWs/GO film as well as the reduced CuNWs network and rGO films have been measured by photoemission spectroscopy in air (PESA) yielding IE values of 4.90 ± 0.02 eV, 4.82 ± 0.02 eV and 4.83 ± 0.04 eV, respectively. The IE value of the hybrid film is therefore very similar to the text-book one of graphene (Figure S5).

We have tested the stability of the electrical resistance of our reduced CuNWs/rGO films on PET under bending both in static and dynamic configuration (see SI paragraph 4). Figure 3d shows the electrical resistance of the film for different bending radii, indicating that the sheet resistance is stable up to a r_b of 5 mm and then rapidly increases up to $\sim 73 \Omega/sq$ for a bending

radius of 1.5 mm. The resistance stability for repeated bending cycles displays a sheet resistance change $< 4\%$ after 10,000 bends at a bending radius of 1 cm.

Finally, we have exploited our reduced CuNWs/rGO films, supported on PET substrate, as transparent electrodes in electrochromic devices. As electrochromic material we have chosen poly(3,4-ethylenedioxythiophene) (PEDOT) because of (i) it is cost-effective and easily accessible, (ii) it exhibits very high color contrast and large coloration efficiencies^[26], and (iii) it can be processed using printing techniques typical of industrial scale onto different types of substrates^[27-29]. These features make PEDOT ideal component for large-scale electrochromic devices applications. We have spray-coated PEDOT on the surface of complementary electrodes which were then assembled using the established architecture for electrochromic devices (ECD)^[30-31] with an UV-curable electrolyte layer. Once assembled, the ECDs were characterized by spectroelectrochemical analysis. Here the applied voltages are -1.5 V (reduction of PEDOT) and 0 V (oxidized PEDOT, almost uncolored). These ECDs show the well-known color development of PEDOT, *i.e.* the appearance of an intense blue color at -1.5 V with an absorption spectrum peaking at 623 nm, with an absorption change amounting to 0.16. Significantly, our device exhibited a rather fast switching (about 0.5 s) for both coloration and bleaching processes, which can be ascribed to the high electronic coupling between the conducting layer and PEDOT. Coloration efficiencies are remarkably high ($948 \text{ cm}^2 \text{ C}^{-1}$) for a spray-casted ECD, in line with the best results reported using glass/ITO systems (maximum values are about $1000 \text{ cm}^2 \text{ C}^{-1}$)^[32-33]. Coloration (Q_c) and bleaching (Q_b) electric currents are experimentally the same, being a mandatory characteristic for stable ECD, in order to avoid secondary electrochemical reactions.

To prove the relevance of our devices for technological applications, and in particular to test its resistance to its operation, we have run it for several days the device^[32] by performing 5 seconds electrochemical cycles in a custom-made chamber described in the experimental

section. Digital photographic images of the devices were acquired over time with a frequency of 100 ms. To analyze those images, colorimetric CIE L^*a^*b coordinates are determined for the region where the electrochromism develops on the device, which renders 3 different coordinates (L^* for luminosity, a^* for red/green color balance, and b^* for yellow/blue color balance). A color contrast is then measured between *off* (bleached) and *on* (colored) states for a given electrochromic cycle. The so-called color contrast parameter, ΔE^* , is in fact a root-mean squared color deviation from the *off* state, and it is in close contact to what the human eye experiences: if it is higher than 3 ($\Delta E^* > 3$) the color change is detectable.^[31-32] This parameter may be followed during the switch, enabling the calculation of switching times for some given cycle number. Significantly, for about 1000 cycles ΔE^* and switching times maintain basically the same performance in terms of color contrast and switching times as the pristine ECD, which is a remarkable result. Afterwards 1,000 cycles, the ECD still operates with fast switching times and color contrasts. Interestingly, at about 20,000 cycles the color contrast was about 50% of the initial value, which ensures very high stability of the electrodes. The coloration efficiency amounts to $174 \text{ cm}^2 \text{ C}^{-1}$ after those 20,000 cycles, being still very high even when compared even with pristine ECDs, providing unambiguous evidence for the robustness of our device.

Such results suggest that rGO is acting as an effective barrier between the electroactive material and the CuNWs network allowing redox reaction to take place. However, the presence of some uncoated area may be the cause of the progressive decomposition of the CuNWs network which is reflected in the increase of the switching time observed in the electrochromic device after over 1,000 cycles.

The highly conducting and transparent hybrid CuNWs/rGO electrodes reported in this paper can be processed/printed using methods like ink-jet or spray which enable the simple preparation of large-area electrodes also supported on flexible substrates. As a proof-of-

concept, high performance ECD has been fabricated and characterized. The robustness and chemical stability of the electrodes also after several voltage cycling when in contact with an electrolyte, promotes these hybrid materials for the replacement of ITO in different optoelectronic applications such as organic light emitting diodes (OLEDs) and organic photovoltaics (OPVs), but also for biomedical applications such as disposable electrodes for electrochemiluminescence (ECL) biosensing and immunoassay applications.

Experimental Section

See Supporting Information.

Supporting Information

Supporting Information is available from the Wiley Online Library or from the author.

As supporting file the movie of an electrochromic device (supported on PET) in action by sweeping the voltage between -1.5 and 0 volts is displayed.

Acknowledgements

We acknowledge financial support by the European Commission through the FP7-NMP-2012-SMALL-6 “SACS” project (GA-310651), the Graphene Flagship (GA-696656), as well as the IRTG Soft Matter Science and the Agence Nationale de la Recherche through the LabEx CSC (ANR-10-LABX-0026_CSC) and the International Center for Frontier Research in Chemistry (icFRC). This work also was supported by the Associated Laboratory for Sustainable Chemistry- Clean Processes and Technologies- LAQV which is financed by national funds from FCT/MEC (UID/QUI/50006/2013) and co-financed by the ERDF under the PT2020 Partnership Agreement (POCI-01-0145-FEDER – 007265).

Received: ((will be filled in by the editorial staff))

Revised: ((will be filled in by the editorial staff))

Published online: ((will be filled in by the editorial staff))

References

- [1] Arias, A. C.; MacKenzie, J. D.; McCulloch, I.; Rivnay, J.; Salleo, A., *Chem. Rev.* **2010**, *110*, 3-24.
- [2] Liu, Z.; Parvez, K.; Li, R.; Dong, R.; Feng, X.; Müllen, K., *Adv. Mater.* **2015**, *27*, 669-675.
- [3] Ye, S.; Rathmell, A. R.; Chen, Z.; Stewart, I. E.; Wiley, B. J., *Adv. Mater.* **2014**, *26*, 6670-6687.
- [4] Parvez, K.; Li, R.; Puniredd, S. R.; Hernandez, Y.; Hinkel, F.; Wang, S.; Feng, X.; Müllen, K., *ACS Nano* **2013**, *7*, 3598-3606.
- [5] Pang, S.; Hernandez, Y.; Feng, X.; Müllen, K., *Adv. Mater.* **2011**, *23*, 2779-2795.
- [6] Quintana, M.; Vazquez, E.; Prato, M., *Acc. Chem. Res.* **2013**, *46*, 138-148.
- [7] Rathmell, A. R.; Wiley, B. J., *Adv. Mater.* **2011**, *23*, 4798-4803.
- [8] Jin, M.; He, G.; Zhang, H.; Zeng, J.; Xie, Z.; Xia, Y., *Angew. Chem. Int. Ed.* **2011**, *50*, 10560-10564.
- [9] Li, S.; Chen, Y.; Huang, L.; Pan, D., *Inorg. Chem.* **2014**, *53*, 4440-4444.
- [10] Kevin, M.; Lim, G. Y. R.; Ho, G. W., *Green Chem.* **2015**, *17*, 1120-1126.
- [11] Won, Y.; Kim, A.; Lee, D.; Yang, W.; Woo, K.; Jeong, S.; Moon, J., *NPG Asia Mater* **2014**, *6*, e105.
- [12] Ding, S.; Jiu, J.; Gao, Y.; Tian, Y.; Araki, T.; Sugahara, T.; Nagao, S.; Nogi, M.; Koga, H.; Sukanuma, K.; Uchida, H., *ACS Appl. Mater. Interfaces* **2016**, *8*, 6190-6199.
- [13] Rathmell, A. R.; Nguyen, M.; Chi, M.; Wiley, B. J., *Nano Lett.* **2012**, *12*, 3193-3199.
- [14] Chen, Z.; Ye, S.; Stewart, I. E.; Wiley, B. J., *ACS Nano* **2014**, *8*, 9673-9679.
- [15] Hsu, P.-C.; Wu, H.; Carney, T. J.; McDowell, M. T.; Yang, Y.; Garnett, E. C.; Li, M.; Hu, L.; Cui, Y., *ACS Nano* **2012**, *6*, 5150-5156.
- [16] Shi, L.; Wang, R.; Zhai, H.; Liu, Y.; Gao, L.; Sun, J., *Phys. Chem. Chem. Phys.* **2015**, *17*, 4231-4236.
- [17] Chen, S.; Brown, L.; Levendorf, M.; Cai, W.; Ju, S.-Y.; Edgeworth, J.; Li, X.; Magnuson, C. W.; Velamakanni, A.; Piner, R. D.; Kang, J.; Park, J.; Ruoff, R. S., *ACS Nano* **2011**, *5*, 1321-1327.
- [18] Ahn, Y.; Jeong, Y.; Lee, D.; Lee, Y., *ACS Nano* **2015**, *9*, 3125-3133.
- [19] Pei, S.; Cheng, H.-M., *Carbon* **2012**, *50*, 3210-3228.
- [20] Yang, D.; Velamakanni, A.; Bozoklu, G.; Park, S.; Stoller, M.; Piner, R. D.; Stankovich, S.; Jung, I.; Field, D. A.; Ventrice Jr, C. A.; Ruoff, R. S., *Carbon* **2009**, *47*, 145-152.
- [21] Zhang, J.; Yang, H.; Shen, G.; Cheng, P.; Zhang, J.; Guo, S., *Chem. Commun.* **2010**, *46*, 1112-1114.

- [22] Chua, C. K.; Pumera, M., *Chem. Soc. Rev.* **2014**, *43*, 291-312.
- [23] Kholmanov, I. N.; Domingues, S. H.; Chou, H.; Wang, X.; Tan, C.; Kim, J.-Y.; Li, H.; Piner, R.; Zabin, A. J. G.; Ruoff, R. S., *ACS Nano* **2013**, *7*, 1811-1816.
- [24] Rathmell, A. R.; Bergin, S. M.; Hua, Y.-L.; Li, Z.-Y.; Wiley, B. J., *Adv. Mater.* **2010**, *22*, 3558-3563.
- [25] Shin, H.-J.; Kim, K. K.; Benayad, A.; Yoon, S.-M.; Park, H. K.; Jung, I.-S.; Jin, M. H.; Jeong, H.-K.; Kim, J. M.; Choi, J.-Y.; Lee, Y. H., *Adv. Funct. Mater.* **2009**, *19*, 1987-1992.
- [26] Monk, P.; Mortimer, R.; Rosseinsky, D., *Electrochromism and Electrochromic Devices*. Cambridge University Press: 2007.
- [27] Gomes, L.; Marques, A.; Branco, A.; Araújo, J.; Simões, M.; Cardoso, S.; Silva, F.; Henriques, I.; Laia, C. A. T.; Costa, C., *Displays* **2013**, *34*, 326-333.
- [28] Gomes, L.; Branco, A.; Moreira, T.; Feliciano, F.; Pinheiro, C.; Costa, C., *Sol. Energy Mater. Sol. Cells* **2016**, *144*, 631-640.
- [29] C. Costa, N. T., N. Trindade, J. Caldeira, J. Ferra, C. Pinheiro, C.A.T. Laia, *Submitted*.
- [30] Costa, C.; Pinheiro, C.; Henriques, I.; Laia, C. A. T., *ACS Appl. Mater. Interfaces* **2012**, *4*, 1330-1340.
- [31] Costa, C.; Pinheiro, C.; Henriques, I.; Laia, C. A. T., *ACS Appl. Mater. Interfaces* **2012**, *4*, 5266-5275.
- [32] Fonseca, S. M.; Moreira, T.; Parola, A. J.; Pinheiro, C.; Laia, C. A. T., *Sol. Energy Mater. Sol. Cells* **2017**, *159*, 94-101.
- [33] Wu, C. G.; Lu, M. I.; Chang, S. J.; Wei, C. S., *Adv. Funct. Mater.* **2007**, *17*, 1063-1070.

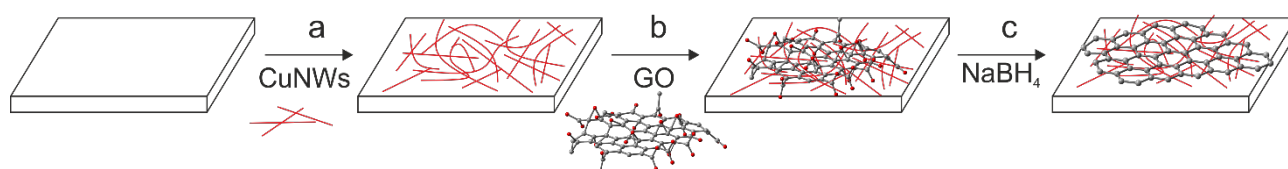


Figure 1. Schematic representation of the preparation of the electrodes. Spray-coating deposition of (a) CuNWs and (b) GO, followed by (c) chemical reduction of the hybrid coating using NaBH₄.

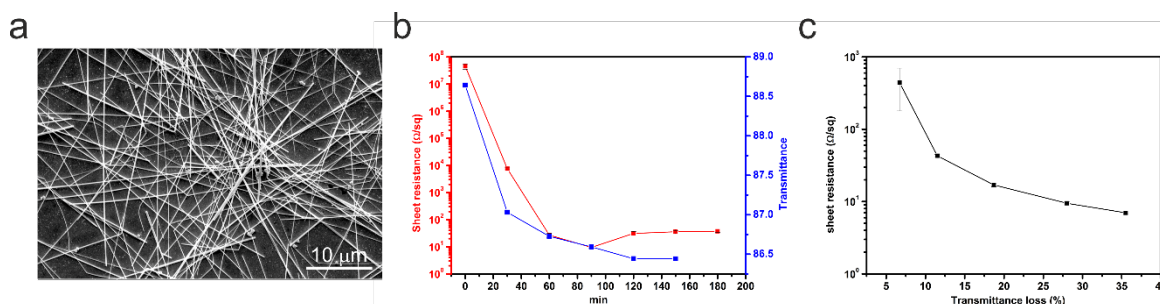


Figure 2. Reduction kinetics and electronic properties of the components. (a) SEM of CuNWs on Au coated glass substrate. (b) Influence of aqueous NaBH₄ time treatment on sheet resistance of CuNWs films (red line) and on the light absorption of GO films with thickness < 100 nm (blue line). (c) Sheet resistance of the reduced hybrid coating as a function of transmittance loss.

10 nm ($\lambda_{\text{abs}} = 550$ nm, blue line) supported on APTES treated glass substrate. (c) Effect of the amount of CuNws in terms of transmittance vs electrode sheet resistance ($\lambda_{\text{abs}} = 550$ nm) after 2.5 hours treatment with NaBH_4 .

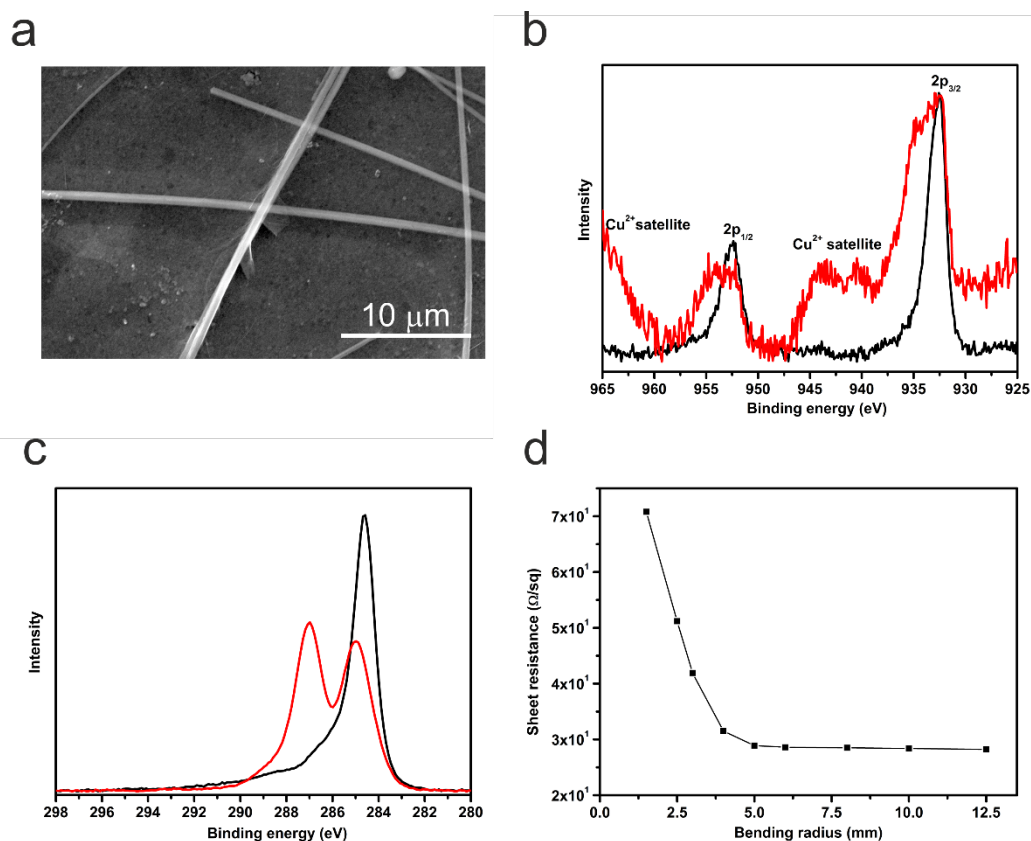


Figure 3. Characterization of the hybrid electrodes. a) SEM of CuNws/rGO after reduction on Au coated glass. XPS analysis of Cu (b) and C (c) of the substrate before (red lines) and after (black lines) reduction with NaBH_4 . (d) Sheet resistance of a reduced CuNws/rGO electrode as a function of the bending radius.

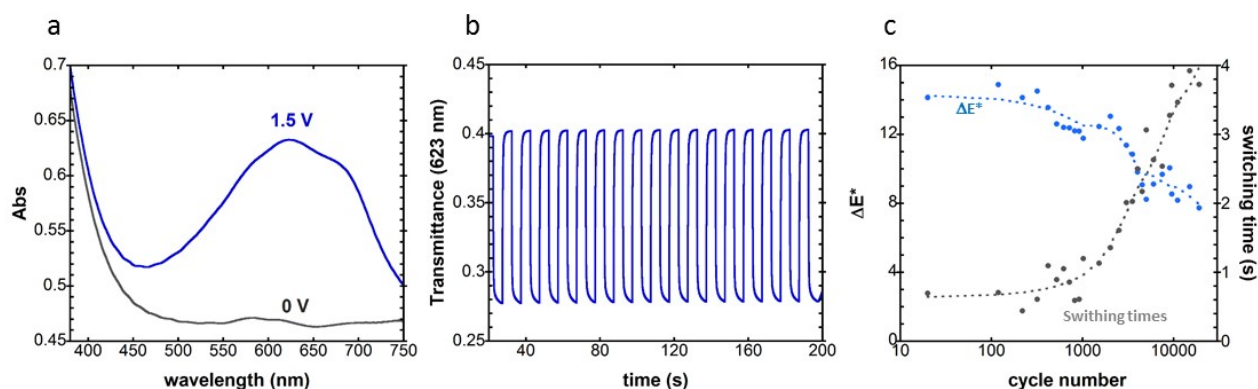


Figure 4. Electrochromic device prototype. (a) Absorption spectra of the ECD with different applied voltages, (b) electrochemical cycling between -1.5 V and 0 V of the ECD followed by optical transmittance at 623 nm, and (c) color contrast (ΔE^*) and switching times of the ECDs measured during the durability test.

Table 1. Figure of merits of the opto-electronic properties of the hybrid films as a function of the number of cycles in the electrochromic device. $\Delta\text{Abs}^{\text{max}}$ is the maximum absorbance change at 623 nm, coloration (Q_c) and bleaching (Q_b) electric current, coloration efficiency (CE, measured after 95% change of optical transmittance) and switching time for colored (τ_c) and bleached (τ_b) states of the ECDs (also measured after 95% change of optical transmittance).

Number of cycles	$\Delta\text{Abs}^{\text{max}}$	Q_c (mC cm ⁻²)	Q_b (mC cm ⁻²)	CE (cm ² C ⁻¹)	τ_c (s)	τ_b (s)
20	0.160	0.14	0.14	948	0.4	0.4
20000	0.086	1.04	0.45	174	18.9	8.4